

Time-Contrastive Networks: Self-Supervised Learning from Multi-View Observation

Pierre Sermanet* Corey Lynch*† Jasmine Hsu Sergey Levine

sermanet,coreylynch,hellojas,slevine@google.com

Google Brain

Abstract

We propose a self-supervised approach for learning representations entirely from unlabeled videos recorded from multiple viewpoints. This is particularly relevant to robotic imitation learning, which requires a viewpoint-invariant understanding of the relationships between humans and their environment, including object interactions, attributes and body pose. We train our representations using a triplet loss, where multiple simultaneous viewpoints of the same observation are attracted in the embedding space, while being repelled from temporal neighbors which are often visually similar but functionally different. This signal encourages our model to discover attributes that do not change across viewpoint, but do change across time, while ignoring nuisance variables such as occlusions, motion blur, lighting and background. Our experiments demonstrate that such a representation even acquires some degree of invariance to object instance. We demonstrate that our model can correctly identify corresponding steps in complex object interactions, such as pouring, across different videos with different instances. We also show what is, to the best of our knowledge, the first self-supervised results for end-to-end imitation learning of human motions by a real robot. Results are best visualized in videos available at¹.

1. Introduction

While supervised learning has been successful on a range of tasks where labels can easily be specified by humans, such as object classification, many problems that arise in interactive applications like robotics are exceptionally difficult to supervise. For example, it would be impractical to label every aspect of a pouring task in enough detail to allow a robot to understand all the task-relevant properties. Pouring demonstrations could vary in terms of background,

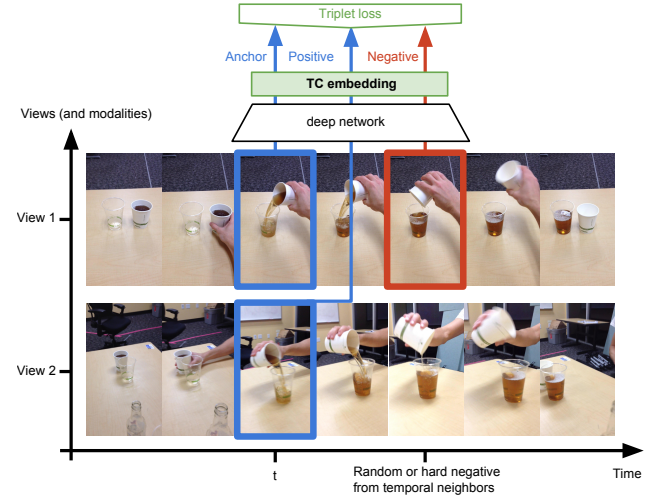


Figure 1: Time-Contrastive Networks (TCN): Anchor and positive images taken from simultaneous viewpoints are encouraged to be close in the embedding space, while distant from negative images taken from a different time in the same sequence. This forces the model to capture properties that vary over time but are consistent across views, such as pose, while becoming invariant to irrelevant transformations such as background or lighting.

containers, and viewpoint, and there could be many salient attributes in each frame, e.g. whether or not a hand is contacting a container, the tilt of the container, or the amount of liquid currently in the target vessel or its viscosity. Ideally, robots in the real world would be capable of two things: first, the ability to learn the relevant properties of an interaction purely from observation; second, the ability to solve a difficult correspondence problem[2] between humans and robots, and imitate human behavior directly from *third-person observation*. In this work we propose a *self-supervised approach* that addresses both of these problems simultaneously, learning representations suitable for understanding object interaction and enabling robotic imitation of a human. We obtain a learning signal from unlabeled multi-viewpoint videos of the same scene, as illustrated in Figure 1, and show that the learned representations effectively disentangle functional attributes like

*equal contribution

†Google Brain Residency program (g.co/brainresidency)

¹sermanet.github.io/tcn

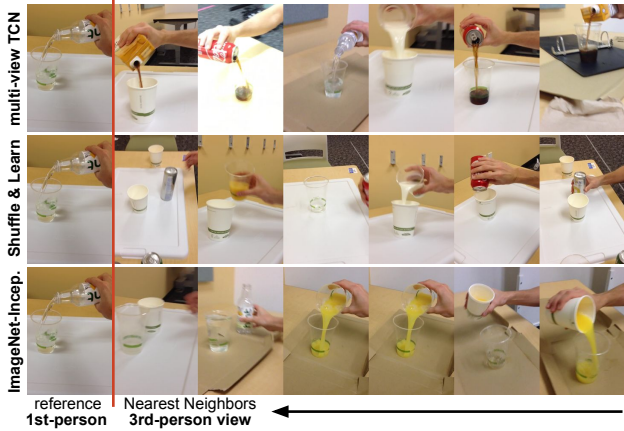


Figure 2: **Label-free pouring imitation:** nearest neighbors (right) for each reference image (left) for different models (multi-view TCN, Shuffle & Learn and ImageNet-Inception). These pouring test images show that the **TCN model can distinguish different hand poses and amounts of poured liquid simply from unsupervised observation** while being invariant to viewpoint, background, objects and subjects, motion-blur and scale.

pose from viewpoint and agent. Then we show how the imitator can learn to link this visual representation to a corresponding motor representation via self-supervised regression, resulting in end-to-end imitation without human pose labels.

In contrast to most prior work on self-supervised representation learning, our aim is not to acquire good representations for semantic classification, detection, or segmentation tasks. Rather we build on good existing representations (e.g. features of networks trained for ImageNet classification) to improve their ability to discriminate interactions between objects, humans, and their environment while maintaining invariance to nuisance variables such as viewpoint and appearance. To that end, we learn our representations on top of features trained for ImageNet classification, such as the Inception model [4, 26]. Since these models already have semantically relevant features, evaluating them on semantic tasks such as recognition is not a meaningful metric of the performance of our method. Instead, we evaluate our representations on tasks that stress the importance of understanding interaction and movement: classifying the stages of a pouring task, understanding the temporal phases of manipulation tasks, and imitating human motion by a robot.

The contributions of this paper are:

- Introducing an unsupervised learning model capable of representing human/object interactions while learning invariance to viewpoint, occlusions, motion-blur, lighting, background or instance.

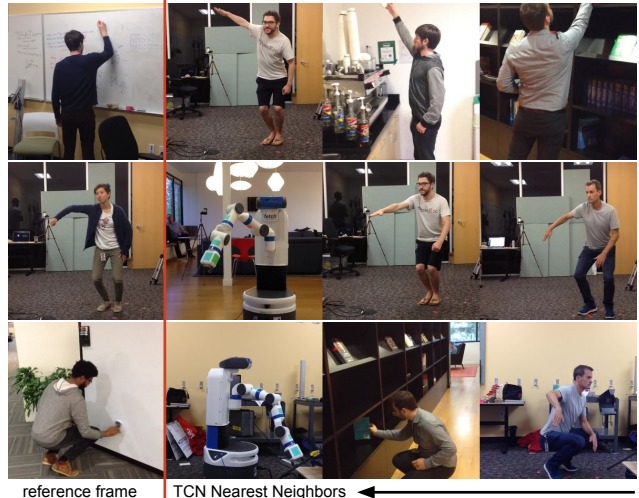


Figure 3: **Label-free pose imitation:** nearest neighbors (right) for each reference frame (left) for each row. Although only trained with self-supervision (no human labels), the multi-view TCN can understand correspondences between humans and robots for poses such as crouching, reaching up and others while being invariant to viewpoint, background, subjects and scale.

- Experimentally demonstrating the value of multi-view correspondence over various single-view signals.
- Reporting the first results for self-supervised end-to-end robotic imitation of human pose (without any labels or explicit representation of human pose).

2. Related Work

Label-free training signals: Label-free learning of visual representations promises to enable visual understanding from unsupervised data, and therefore has been explored extensively in recent years. Prior work in this area has studied unsupervised learning as a way of enabling supervised learning from small labeled datasets [7], image retrieval [18], and a variety of other tasks [28, 35, 12, 27, 20, 10]. In this paper, we focus specifically on representation learning for the purpose of model interactions between objects, humans, and their environment, which requires implicit modeling of a broad range of factors, such as functional relationships, while being invariant to nuisance variables such as viewpoint and appearance. In evaluating our approach, we test its ability to uncover corresponding steps between different executions of the same task and its applicability to robotic imitation of human movements. Our method makes use of simultaneously recorded signals from multiple viewpoints to construct an image embedding. A number of prior works have used multiple modalities and temporal or spatial coherence to extract embeddings and features. For example, [16, 1] used co-occurrence of sounds and visual cues in videos to learn meaningful visual fea-

tures. [35] also propose a multi-modal approach for self-supervision by training a network for cross-channel input reconstruction. While similar, our approach is simpler in that it does not require low-level generation of each modality (i.e. pixel-level reconstruction). [5, 33] use the spatial coherence in images as a self-supervision signal, [17] use motion cues to self-supervise a segmentation task, and [34] use camera pose estimation and feature matching. These methods are more focused on spatial relationships, and the unsupervised signal they provide is complementary to the one explored in this work.

A number of prior works use temporal coherence [31, 11, 8, 14]. Others also train for viewpoint invariance using metric learning [10, 32, 23]. The novelty of our work is to combine both aspects in opposition, as explained in Sec. 3.1. [28] uses a triplet loss that encourages first and last frames of a tracked sequence to be closer together in the embedding, while random negative frames from other videos are far apart. Our method differs in that we use temporal neighbors as negatives to push against a positive that is anchored by a simultaneous viewpoint. This causes our method to discover meaningful dimensions such as attributes or pose, while [28] focuses on learning intraclass invariance. Simultaneous multi-view capture also provides exact correspondence while tracking does not, and can provide a rich set of correspondences such as occlusions, blur, lighting and viewpoint.

Other works have proposed to use prediction as a learning signal [29, 13]. The resulting representations are typically evaluated primarily on the realism of the predicted images, which remains a challenging open problem. In contrast, our method can use a simple triplet loss for supervision, and our evaluation shows that it can produce semantically meaningful nearest neighbors for a variety of object interaction scenarios. A number of other prior methods have used a variety of labels and priors to learn embeddings. [15] use a labeled dataset to train a pose embedding, then find the nearest neighbors for new images from the training data for a pose retrieval task. Our method is initialized via ImageNet training, but can discover dimensions such as pose and task progress (e.g., for a pouring task) without any task-specific labels. [25] explore various types of physical priors, such as the trajectories of objects falling under gravity, to learn object tracking without explicit supervision. Our method is similar in spirit, in that it uses temporal co-occurrence, which is a universal physical property, but the principle we use is general and broadly applicable and does not require task-specific input of physical rules.

Imitation learning: In the context of robotics and reinforcement learning, prior works have also considered the problem of imitating a demonstration observed from a different viewpoint or from an agent with a different embodiment, such as a human [24, 6, 22]. Although our approach

is not specific to imitation learning and focuses on general-purpose representation learning, our robotic experiments show that it is imminently applicable to imitating human movements due to the viewpoint invariance and body pose sensitivity acquired automatically by the model.

Mirror Neurons: Humans and animals have been shown, experimentally, to possess viewpoint-invariant representations of objects and other agents in their environment [3], and the well known work on “mirror neurons” has demonstrated that these viewpoint invariant representations are crucial for imitation [19]. Our multi-view capture setup in Fig. 4 is similar to the experimental setup used by [3], and our robot imitation setup, where a robot imitates human motion without ever receiving ground truth pose labels, examines how self-supervised pose recognition might arise in a learned system.

3. Approach

3.1. Multi-View Time-Contrastive Supervision

We illustrate our approach, which we call time-contrastive (TC) supervision, in Fig. 1. The method uses multi-view metric learning via a triplet loss [21]. The core idea is that two frames (anchor and positive) coming from the same time but different viewpoints (or modalities) are pulled together, while a visually similar frame from a temporal neighbor is pushed apart. The TC signal serves multiple purposes. First, the **cross-view correspondence encourages learning invariance to viewpoint, scale, occlusion, motion-blur, lighting and background**, since the positive and anchor frames show the same subject with variation along these factors. For example, Fig. 1 exhibits all these transformations between the top and bottom sequences except for occlusion. An example of occlusion correspondence is shown in Fig. 17. Learning a rich set of invariances is useful for vision in general, but we are particularly interested in viewpoint invariance for understanding object interactions and imitating human motion, as discussed in Sec. 5. Second, the **TC signal introduces competition between temporal neighbors** to explain away visual changes over time. For example, in Fig. 1, because neighbors are so similar visually, the only way to tell them apart is to model the amount of liquid present in the cup, or to model the pose of hands or objects and their interactions. The key ingredient in our approach is that **multi-view pairs ground and disambiguate the possible explanations for changes in the physical world**. We show in Sec. 4 and Sec. 5 that TCN can indeed discover correspondences based on object interactions, object, and body poses, as well as attributes such as liquid levels in cups and pouring stages, all in a self-supervised manner. Additionally, and perhaps surprisingly, we find that TCNs can learn cross-class invariance even though **no explicit correspondence**

between subjects was ever provided. This is demonstrated by the quantitative improvements in imitation of humans not seen during training (see Sec. 5.4.1). The unsupervised correspondences found between humans and robot is another example. For qualitative examples, the nearest neighbors shown in Fig. 2 and Fig. 3 exhibit similar states and attributes while being invariant to the instance of the human subject or object. We hypothesize the cross-class alignment naturally falls into place in the TC embedding because when anchor and positive pairs consistently have very little low level visual similarity (as is the case in the multi-view context), more abstract and view-independent properties such as pose are the only regularities that the model can consistently exploit. And sharing the learned dimensions across different instances offers the most efficient embedding organization. Additionally, some visual commonalities across classes may contribute to this phenomenon.

Multi-view data collection is simple and can be captured with as little as two operators equipped with smartphones, as shown in Fig. 4. One operator keeps a fixed point of view of the region of interest while performing the task, while the other moves the camera freely to introduce the rich set of variations discussed above. While more cumbersome than single-view capture, we argue that multi-view capture is cheap, simple, and practical, when compared to alternatives such as human labeling.



Figure 4: **Multi-view capture** with two operators equipped with smartphones. Moving the cameras around freely introduces a rich variety of scale, viewpoint, motion-blur and background correspondences between the two cameras.

3.2. Single-View TCN

We can also consider time-contrastive models trained on single-view video as shown in Fig. 5. In this case, the positive frame is randomly selected within a certain range of the anchor. A margin range is then computed given the positive range. Negatives are randomly chosen outside of the margin range and the model is trained as before.

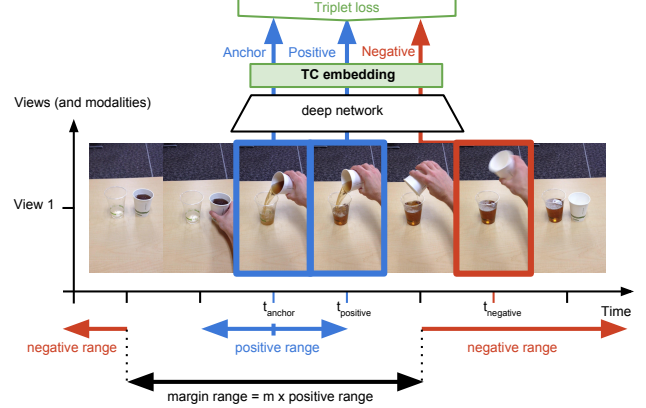


Figure 5: **Single-view TCN:** positives are selected within a small window around anchors, while negatives are selected from distant timesteps in the same sequence.

4. Objects Interactions Experiments

4.1. Liquid Pouring

In this experiment, we study what a TCN can capture simply by observing a human subject pouring liquids from different containers into different cups. The videos were captured using two standard smartphones (see Fig. 4), one from a subjective point of view by the human performing the pouring, and the other from a freely moving third-party viewpoint. Capture is synchronized across the two phones using an off-the-shelf app and each sequence is approximately 5 seconds long. We divide the collected videos in two sets: 180 videos for training (about 15 minutes total) and 30 for testing. The training videos contain clear and opaque cups, but we restrict the testing videos to clear cups only in order to evaluate if the model has an understanding of how full the cups are.

4.1.1 Models

In all experiments, we use the following custom architecture derived from the Inception architecture [26]. It consists of the Inception model up until the layer “Mixed_5d” (initialized with ImageNet pre-trained weights), followed by 2 convolutional layers, a spatial softmax layer [9] and a fully-connected layer. The embedding is a fully connected layer with 128 units added on top of our custom model. This embedding can be trained either with the multi-view TC loss (as shown in Fig. 1), the single-view TC loss or the Shuffle & Learn loss[14]. For the TCN models, we use the triplet loss from [21] without modification and with a gap value of 0.2. Note that in all experiments below, negatives always come from the same sequence as positives. We use the output of the last layer before the classifier of an ImageNet-pretrained Inception model [4, 26] (a 2048-dimensional vector) as a baseline in the following experi-

ments, and call it "Inception-ImageNet". Since the custom model is initialized from ImageNet pre-training, it is a natural point of comparison which allows us to control for any invariances that are introduced through ImageNet training rather than other approaches.

We compare TCN models to a Shuffle & Learn [14] model trained on our data, using the same hyper-parameters taken from the paper (t_{\max} of 60, t_{\min} of 15, and negative class ratio of 0.75). Note that in our implementation, neither the Shuffle & Learn baseline nor TCN benefit from a biased sampling to high-motion frames. To directly measure the effects of multi-view over single-view, we compare to a single-view TCN, with a positive range of 0.2 seconds and a negative multiplier of 2.

4.1.2 Quantitative Evaluation

In this section, all results are based on nearest neighbors to a reference frame in the embedding space of each model. We define a "Random" baseline by returning a random frame instead of a nearest neighbor. We explore multiple metrics in Table 1 to analyze the performance of different models. First, we define a sequence alignment metric which is particularly relevant and important when learning to imitate, especially from a third-party perspective. For each pouring test video, a human operator labels the key frames corresponding to the following events: first frame with hand contact with pouring container, first frame where liquid is flowing, last frame where liquid is flowing and last frame with hand contact with the container. These keyframes establish a coarse semantic alignment which should provide a relatively accurate piecewise-linear correspondence between all videos. For any pair of videos (v_1, v_2) in the test set, we embed each frame given the model to evaluate. For each frame of the source video v_1 , we associate it with its nearest neighbor in embedding space taken from all frames of v_2 . We evaluate how well the nearest neighbor in v_2 semantically aligns with the reference frame in v_1 . Thanks to the labeled alignments, we find the proportional position of the reference frame with the target video v_2 , and compute the frame distance to that position, normalized by the target segment length. In Table 1, we find that the TCN models outperform all baselines and that multi-view TCN in particular consistently performs best. Note that in this experiment we evaluate the alignment between similar and different viewpoints.

Second, we define an attribute classification task and label a groundtruth set with the following attributes reported in Fig. 6: is the hand in contact with the container? (yes or no); is the container within pouring distance of the recipient? (yes or no); what is the tilt angle of the pouring container? (values 90, 45, 0 and -45 degrees); is the liquid flowing? (yes or no); does the recipient contain li-

Method	alignment err.	classification err.
Random	$28.1\% \pm 3.0$	54.2%
Inception-ImageNet	$27.1\% \pm 7.7$	48.4%
Shuffle & Learn[14]	$21.6\% \pm 6.0$	31.0%
single-view TCN	$20.2\% \pm 6.6$	26.8%
multi-view TCN	$16.3\% \pm 5.6$	20.2%

Table 1: **Pouring alignment and classification errors:** TCN models outperform all baselines on both metrics. The classification error considers 5 classes related to pouring: "hand contact with recipient", "within pouring distance", "container angle", "liquid is flowing" and "recipient fullness".

uid? (yes or no). These particular attributes are evaluated because they matter for imitating and performing a pouring task. We compare with the Inception-2048 baseline as above as well as a random baseline. Naturally, classification results are normalized by class distribution. We observe that the multi-view TCN reduces the error by 35% on average compared to the Shuffle & Learn baseline. Note that while this could be compared to a supervised classifier, as mentioned in the introduction, it is not realistic to expect labels for every possible task in a real application, e.g. in robotics. Instead, in this work we aim to compare to realistic general off-the-shelf models that one might use without requiring new labels.

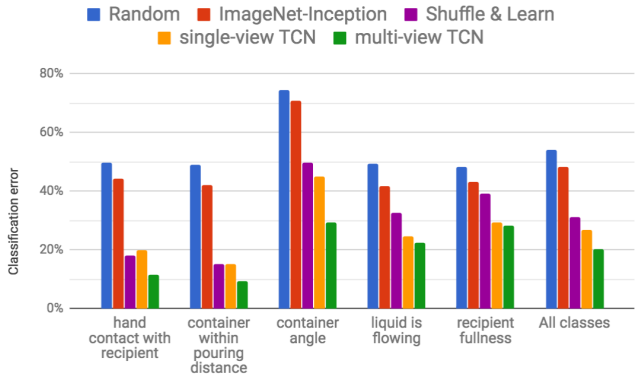


Figure 6: **Attributes classification error:** TCN models outperform baselines, the multi-view TCN performs best.

4.1.3 Qualitative Evaluation

In Fig. 2, we present k-Nearest-Neighbors (kNN) for each reference frame. We see that neighbors are semantically similar, despite visual differences in pouring containers, different viewpoints and different recipients. We encourage readers to refer to supplementary videos to better grasp these results. More kNN examples as well as t-SNE visualizations of the embedding are available in Sec. A.

5. End-to-end Pose Imitation Experiment

We apply multi-view TCN to the problem of human pose imitation by a robot, as depicted in Fig. 7. Multi-view TCN is particularly well suited for this task because in addition to requiring viewpoint and robot/human invariance, the correspondence problem is ill-defined and difficult to supervise. In this section, we describe the necessary additions (signals, data, models and metrics) for this application. Apart from adding a few layers on top of the TC embedding as described in Sec. 5.1, there is no fundamental difference between this section and the previous one, i.e. humans can be seen as objects with many degrees of freedom or attributes to be discovered by our self-supervised model. Throughout this section, we use the Human Supervision described in Fig. 8 as groundtruth. Human images are fed into the imitation system, and the resulting joints vector is compared to the groundtruth joints vector associated with the human pose. In all experiments, we report the L2 error distance between robot joint vectors collected during human imitation and the predicted ones. The L2 error is normalized by the possible value range of each joint, resulting in a percentage error. Note that the Human Supervision signal is quite noisy because it is a non-trivial task that can be interpreted differently by different human subjects. In fact, a perfect imitation is not possible due to physiological differences between human bodies themselves and the Fetch robot, and the ground truth is highly subjective. Therefore, the best comparison metric available to us is to see whether the joint angles predicted from a held-out human observation match the actual joint angles that the human was attempting to imitate.

5.1. Models

We train our end-to-end robotic imitation model using 3 different signals as described in Sec. 5.2. The model consists of a TCN model as described in Sec. 4.1.1 to which we add a joint decoder network (2 fully-connected layers above TC embedding: $\rightarrow 128 \rightarrow 8$, producing 8 joint values). We train the joints decoder with L2 regression using the self-supervision or the human supervision signals. The model can be trained with different combinations of signals; we study the effects of each combination in section Sec. 5.4.1. At test time, the resulting joints vector can then directly be fed to the robot stack to update its joints as depicted in Fig. 7, resulting in an **end-to-end imitation without any explicit representation of human pose**.

5.2. Training Signals

In this section, we discuss additional signals described in Fig. 8 that can be used in conjunction to the TC signal for imitation: the self-supervision and the human supervision signals. While the TC and self supervision signals are **cheap to collect and provide perfect correspondences**,

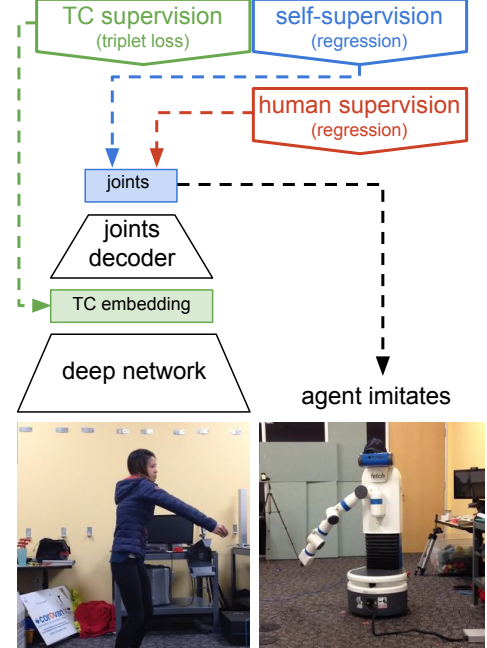


Figure 7: **TCN for end-to-end imitation:** architecture, training and imitation. The embedding is trained unsupervised with the time-contrastive loss, while the joints decoder can be trained with self-supervision, human supervision or both. Produced joints can be used directly by the robot to perform the imitation. Human pose is never explicitly represented.

human supervision is very expensive to collect and comes typically with noisy correspondences. We will show in the rest of the paper that large quantities of cheap supervision can be effectively mixed with small amounts of expensive supervision.

5.2.1 Self-Supervision Signal

Here we describe how the robot uses a self-supervised signal to learn to convert TCN-encoded observations to corresponding joint angles. During self-observation, the robot is presented with a stream $(TCN(X_{robot}), y)$, where $TCN(X_{robot})$ is a TCN-encoded third person observation of itself and y are its internal joint angles that correspond directly to what it observes. This data is used to train a *self-supervised joint decoder* via L2 regression, where the output of the decoder is compared to the robot's actual corresponding joint angles at the time. Together, the TCN encoder and the self-supervised joint decoder allow the robot to *encode human observation, decode corresponding action*. This is shown in Fig. 7. Like with TC supervision, data for the self-supervision signal is very cheap to collect and provides perfect correspondences. While a single camera can be used for this setup, multiple cameras scales the data up and reduces the collection time. Note that the joint

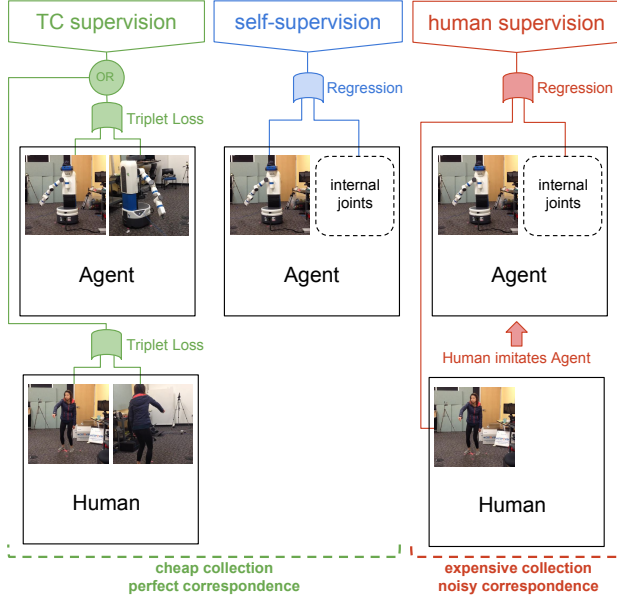


Figure 8: **Training signals for imitation:** TC, self and human supervision. The time-contrastive signals (left) allow the model to learn rich representations of humans or robots individually. The self-supervision signal (center) gives the robot an ability to predict its own joint values given a learned embedding. Finally, the human supervision signal (right) is collected from humans attempting to imitate robot poses.

decoder problem can be trained concurrently with TCN, using the same self-observation data.

5.2.2 Human Supervision Signal

In addition to using human imitation data for a quantitative measure, we can also consider using it as an additional training signal for both the encoder and decoder. We collect human supervision data as follows: the robot performs random motions and records its internal joints, while a human observer captured by multiple cameras attempts to imitate it. This presents the robot with a stream ($TCN(X_{Human}, y)$, where $TCN(X_{Human})$ is the TCN-encoded observation of its human imitator and y are the joint angles being imitated. Unlike the self-supervision data, there's no longer an exact correspondence between observation and joint angles: physiological differences make the imitation non-trivial and subjective to the imitator. We found that, in practice, humans prefer to imitate the functional form of the motion, prioritizing the end-effector over joints that are more difficult to match. We use a Fetch robot[30] in our experiment, which requires a fair amount of training and concentration for humans to imitate. To alleviate the difficulty, we simplify the agent's motion to alternatively move to a random joints position and move a single joint at a time across its entire span. This allows humans to focus on a

single joint, while sampling a varied set of positions. Similarly to the self-supervision signal, this collection can be done with a single camera but can also be scaled up with multiple cameras.

5.3. Data

The human training data consists of sequences distinguished by human subject and clothing pair. Each sequence is approximately 4 minutes. For the label-free TC supervision we collected approximately 30 human pairs (about 2 hours) where humans imitate a robot but the joint labels are not recorded, along with 50 robot sequences with random motion (about 3 hours, trivial to collect). For human supervision, we collected 10 human/clothing pairs (about 40 minutes, very expensive collection) while also recording the joints labels. Each recorded sequence is captured by 3 smartphone cameras fixed on tripods at specific angles (0° , 60° and 120°) and distance. The validation and testing sets each consist of 6 human/clothing pairs not seen during training (about 24 minutes, very expensive collection).

5.4. Quantitative Results

5.4.1 Supervision Analysis

As shown in Fig. 7, our imitation system can be trained with different combinations of signals. Here we study how our self-supervised imitation system compares to the other possible combinations of training signals. The performance of each combination is reported in Table 2 using the maximum amounts of data available (10 sequences for Human supervision and 30 sequences for TC supervision), while Fig. 9 varies the amount of human supervision. Models such as the "TC + Self" or "Self" do not appear as single points on the vertical axis. Models that do not include TC supervision are simply trained as end-to-end regression problems. For example the Self model is trained end-to-end to predict internal joints from third person observations of the robot, and then that model is applied directly to the human imitation task. For reference, we compute a random baseline which samples joints values within physically possible ranges. In general, we observe that more human supervision decreases the L2 robot joints error. It is interesting to note that **while not given any labels, the self-supervised model ("TC + Self") still significantly outperforms the fully-supervised model ("Human")**. The combination of all supervision signals performs the best. Overall, we observe that **adding the TC supervision to any other signal significantly decreases the imitation error**. In Fig. 10, we vary the amount of TC supervision provided and find the imitation error keeps decreasing as we increase the amount of data. Based on these results, we can make the argument that relatively large amounts of cheap weakly-supervised data and small amounts of expensive human supervised data is

an effective balance for our problem. A non-extensive analysis of viewpoint and scale invariance in Sec. C seems to indicate that the model remains relatively competitive when presented with viewpoints and scales not seen during training.

Supervision	L2 robot joints error %
Random (possible) joints	42.4 ± 0.1
Self	38.8 ± 0.1
Human	33.4 ± 0.4
Human + Self	33.0 ± 0.5
TC + Self	32.1 ± 0.3
TC + Human	29.7 ± 0.1
TC + Human + Self	29.5 ± 0.2

Table 2: **Imitation error for different combinations of supervision signals.** The error reported is the L2 robot joints distance between prediction and groundtruth, as a percentage error normalized by the possible range of each joint. Note that no perfect imitation is possible.

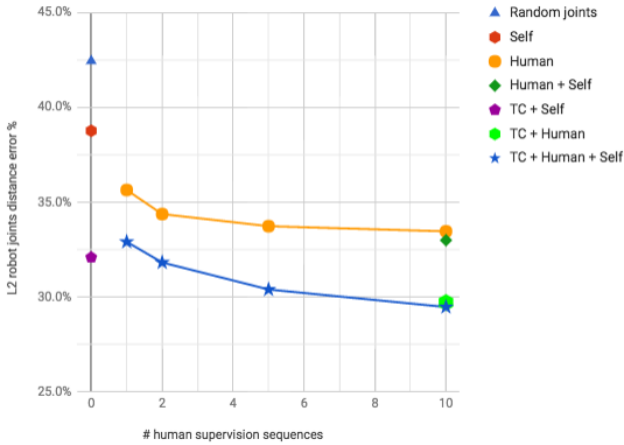


Figure 9: **Comparing types and amounts of supervision:** we measure the L2 joints error, i.e. imitation error, while varying the combinations of supervision between Self, Human and TC against a random baseline. We also vary the amount of human supervision (horizontal axis).

5.4.2 Analysis by Joint

In Fig. 11, we examine the error of each joint individually for 4 models. Interestingly, we find that for all joints excepts for "shoulder pan", the unsupervised "TC+Self" models performs almost as well as the human-supervised "TC+Human+Self". The unsupervised model does not seem to correctly model the shoulder pan and performs worse than Random. Hence most of the benefits of human supervision found in Fig. 9 come from correcting the shoulder pan prediction.

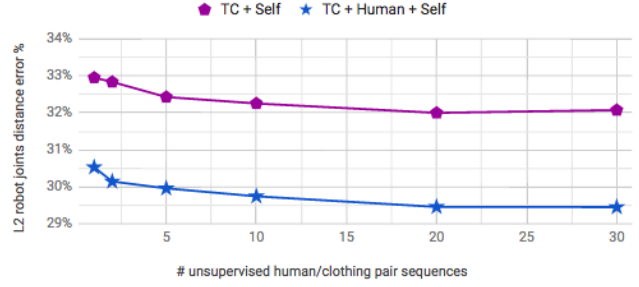


Figure 10: **Varying the amount of unsupervised data:** increasing the number of unsupervised sequences decreases the imitation error for both models.

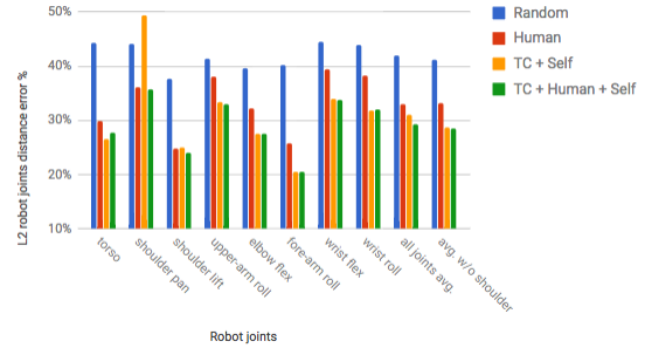


Figure 11: **L2 robot error break-down by robot joints.** From left to right, we report errors for the 8 joints of the Fetch robot, followed by the joints average, followed by the joints average excluding the "shoulder pan" joint.

5.5. Qualitative Results

We offer multiple qualitative evaluations: k-Nearest Neighbors (kNN) in Fig. 3, imitation strips in Fig. 12 and a t-SNE visualization in Fig. 13. Video strips do not fully convey the quality of imitation, we strongly encourage readers to watch the videos accompanying this paper. **kNN:** In Fig. 3, we show the nearest neighbors of the reference frames for the self-supervised model "TC+Self" (no human supervision). **Although never trained across humans, it learned to associate poses such as crouching or reaching up between humans never seen during training and with entirely new backgrounds**, while exhibiting viewpoint, scale and translation invariance. **Imitation strips:** In Fig. 12, we present an example of how the self-supervised model has learned to imitate the height level of humans by itself (easier to see in supplementary videos) using the "torso" joint (see Fig. 11). This stark example of the complex mapping between human and robot joints illustrates the need for learned mappings, **here we learned a non-linear mapping from many human joints to a single "torso" robot joint without any human supervision**. **t-SNE:** We qualitatively evaluate the arrangement of our learned em-

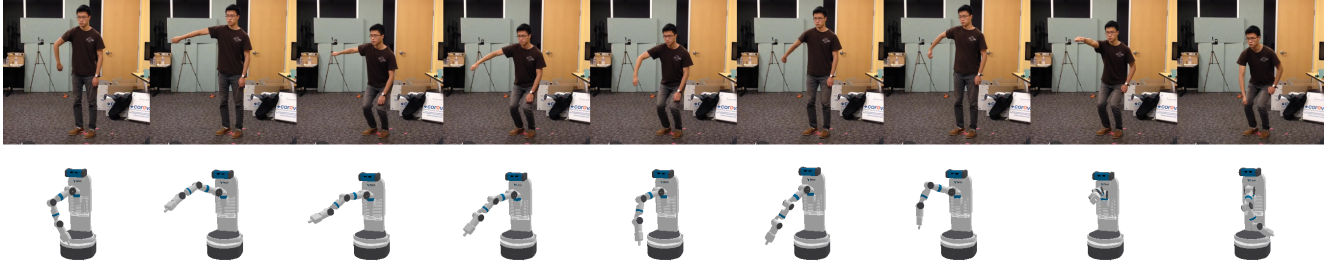


Figure 12: Self-supervised imitation example. Although not trained using any human supervision (model “TC+Self”), the TCN is able to approximately imitate human subjects unseen during training. This example shows that the TCN discovered the mapping between the robot’s torso joint (up/down) and the complex set of human joints commanding crouching. More examples are available in Sec. D.

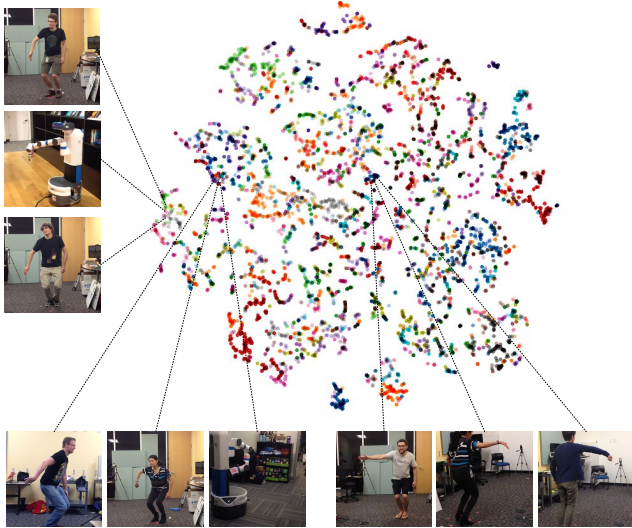


Figure 13: t-SNE embedding colored by agent for model “TC+Self”. We show that images are locally coherent with respect to pose while being invariant to agent or viewpoint.

bedding using t-SNE representations with perplexity of 30 and learning rate of 10. In Fig. 13, we show that the agent-colored embedding exhibits local coherence with respect to pose while being invariant to agent and viewpoint. More kNN examples, imitation strips and t-SNE visualizations from different models are available in Sec. D.

6. Conclusion

We introduced a representation learning method that uses simultaneous views for anchoring a temporally contrastive signal, permitting disambiguation of temporal changes as well as providing invariance to viewpoint and other nuisance variables. We showed that this signal can disentangle object poses, attributes, and interactions in a meaningful way simply from observation. Similarly, we showed that it can uncover different degrees of freedom in humans and robots and associate them across instances, de-

spite never being provided with a correspondence between the joint angles of different subjects. We demonstrated that the learned embedding can be used for end-to-end robotic imitation. An exciting direction for future work is to further investigate the properties and limits of this approach, especially when it comes to understanding what is the minimum degree of viewpoint difference that is required for meaningful representation learning. For example, if we can simply use stereo cameras, data collection would be simplified substantially, and such a result would provide an intriguing insight into how the human visual system might uncover invariances through stereo. Other extensions might involve jointly training heterogeneous modalities, such as stereo audio sensors, force feedback, tactile sensing, infrared sensors, etc., in addition to multiple viewpoints, and examining the kinds of invariances and attributes that would emerge.

Acknowledgments

We would like to thank Jonathan Tompson, James Davidson and Vincent Vanhoucke for helpful discussions and feedback. We are also grateful to Eric Jang and Phing Lee for their repeated help and talent in robot imitation. Finally we thank everyone else who provided imitations for this project: Alexander Toshev, Anna Goldie, Deanna Chen, Deirdre Quillen, Dieterich Lawson, Eric Langlois, Ethan Holly, Irwan Bello, Jasmine Collins, Jeff Dean, Julian Ibarz, Ken Oslund, Laura Downs, Leslie Phillips, Luke Metz, Mike Schuster, Ryan Dahl, Sam Schoenholz and Yifei Feng.

References

- [1] Y. Aytar, C. Vondrick, and A. Torralba. Soundnet: Learning sound representations from unlabeled video. *CoRR*, abs/1610.09001, 2016.
- [2] M. Brass and C. Heyes. Imitation: is cognitive neuroscience solving the correspondence problem? *Trends in cognitive sciences*, 9(10):489–495, 2005.
- [3] V. Caggiano, L. Fogassi, G. Rizzolatti, J. K. Pomper, P. Thier, M. A. Giese, and A. Casile. View-based encoding of actions in mirror neurons of area f5 in macaque premotor cortex. *Current Biology*, 21(2):144–148, 2011.

- [4] J. Deng, W. Dong, R. Socher, L.-J. Li, K. Li, and L. Fei-Fei. ImageNet: A Large-Scale Hierarchical Image Database. In *CVPR09*, 2009.
- [5] C. Doersch, A. Gupta, and A. A. Efros. Unsupervised visual representation learning by context prediction. *CoRR*, abs/1505.05192, 2015.
- [6] A. D. Dragan and S. S. Srinivasa. Online customization of teleoperation interfaces. In *RO-MAN, 2012 IEEE*, pages 919–924. IEEE, 2012.
- [7] V. Dumoulin, I. Belghazi, B. Poole, A. Lamb, M. Arjovsky, O. Mastropietro, and A. Courville. Adversarially learned inference. In *International Conference on Learning Representations (ICLR)*, 2017.
- [8] B. Fernando, H. Bilen, E. Gavves, and S. Gould. Self-supervised video representation learning with odd-one-out networks. *CoRR*, abs/1611.06646, 2016.
- [9] C. Finn, X. Y. Tan, Y. Duan, T. Darrell, S. Levine, and P. Abbeel. Learning visual feature spaces for robotic manipulation with deep spatial autoencoders. *CoRR*, abs/1509.06113, 2015.
- [10] V. K. B. G, G. Carneiro, and I. D. Reid. Learning local image descriptors with deep siamese and triplet convolutional networks by minimizing global loss functions. In *IEEE Conference on Computer Vision and Pattern Recognition, CVPR*, 2016.
- [11] R. Goroshin, J. Bruna, J. Tompson, D. Eigen, and Y. LeCun. Unsupervised learning of spatiotemporally coherent metrics. In *International Conference on Computer Vision (ICCV)*, 2015.
- [12] D. Kingma and M. Welling. Autoencoding variational Bayes. In *International Conference on Learning Representations (ICLR)*, 2014.
- [13] M. Mathieu, C. Couprie, and Y. LeCun. Deep multi-scale video prediction beyond mean square error. *CoRR*, abs/1511.05440, 2015.
- [14] I. Misra, C. L. Zitnick, and M. Hebert. Unsupervised learning using sequential verification for action recognition. *CoRR*, abs/1603.08561, 2016.
- [15] G. Mori, C. Pantofaru, N. Kothari, T. Leung, G. Toderici, A. Toshev, and W. Yang. Pose embeddings: A deep architecture for learning to match human poses. *CoRR*, abs/1507.00302, 2015.
- [16] A. Owens, P. Isola, J. H. McDermott, A. Torralba, E. H. Adelson, and W. T. Freeman. Visually indicated sounds. *CoRR*, abs/1512.08512, 2015.
- [17] D. Pathak, R. B. Girshick, P. Dollár, T. Darrell, and B. Hariharan. Learning features by watching objects move. *CoRR*, abs/1612.06370, 2016.
- [18] M. Paulin, M. Douze, Z. Harchaoui, J. Mairal, F. Perronnin, and C. Schmid. Local convolutional features with unsupervised training for image retrieval. In *International Conference on Computer Vision (ICCV)*, pages 91–99, Dec 2015.
- [19] G. Rizzolatti and L. Craighero. The mirror-neuron system. *Annual Review of Neuroscience*, 27:169–192, 2004.
- [20] R. Salakhutdinov and G. Hinton. Deep Boltzmann machines. In *AISTATS*, 2009.
- [21] F. Schroff, D. Kalenichenko, and J. Philbin. Facenet: A unified embedding for face recognition and clustering. *CoRR*, abs/1503.03832, 2015.
- [22] P. Sermanet, K. Xu, and S. Levine. Unsupervised perceptual rewards for imitation learning. *CoRR*, abs/1612.06699, 2016.
- [23] E. Simo-Serra, E. Trulls, L. Ferraz, I. Kokkinos, P. Fua, and F. Moreno-Noguer. Discriminative learning of deep convolutional feature point descriptors. In *Proceedings of the IEEE International Conference on Computer Vision*, pages 118–126, 2015.
- [24] B. C. Stadie, P. Abbeel, and I. Sutskever. Third-person imitation learning. *arXiv preprint arXiv:1703.01703*, 2017.
- [25] R. Stewart and S. Ermon. Label-free supervision of neural networks with physics and domain knowledge. *CoRR*, abs/1609.05566, 2016.
- [26] C. Szegedy, V. Vanhoucke, S. Ioffe, J. Shlens, and Z. Wojna. Rethinking the inception architecture for computer vision. *CoRR*, abs/1512.00567, 2015.
- [27] P. Vincent, H. Larochelle, Y. Bengio, and P. Manzagol. Extracting and composing robust features with denoising autoencoders. In *International Conference on Machine Learning (ICML)*, 2008.
- [28] X. Wang and A. Gupta. Unsupervised learning of visual representations using videos. *CoRR*, abs/1505.00687, 2015.
- [29] W. F. Whitney, M. Chang, T. D. Kulkarni, and J. B. Tenenbaum. Understanding visual concepts with continuation learning. *CoRR*, abs/1602.06822, 2016.
- [30] M. Wise, M. Ferguson, D. King, E. Diehr, and D. Dymesich. Fetch and freight: Standard platforms for service robot applications. In *Workshop on Autonomous Mobile Service Robots*, 2016.
- [31] L. Wiskott and T. J. Sejnowski. Slow feature analysis: Unsupervised learning of invariances. *Neural Comput.*, 14(4):715–770, Apr. 2002.
- [32] K. M. Yi, E. Trulls, V. Lepetit, and P. Fua. LIFT: learned invariant feature transform. *CoRR*, abs/1603.09114, 2016.
- [33] S. Zagoruyko and N. Komodakis. Learning to compare image patches via convolutional neural networks. In *IEEE Conference on Computer Vision and Pattern Recognition, CVPR 2015, Boston, MA, USA, June 7-12, 2015*, pages 4353–4361, 2015.
- [34] A. R. Zamir, T. Wekel, P. Agrawal, C. Wei, J. Malik, and S. Savarese. Generic 3d representation via pose estimation and matching. In *European Conference on Computer Vision*, pages 535–553. Springer, 2016.
- [35] R. Zhang, P. Isola, and A. A. Efros. Split-brain autoencoders: Unsupervised learning by cross-channel prediction. *CoRR*, abs/1611.09842, 2016.

A. Objects Interaction Analysis

Here, we visualize the embeddings from the ImageNet-Inception and multi-view TCN models with t-SNE using a coloring by groundtruth labels. Each color is a unique combination of 5 attribute values defined earlier, i.e. if each color is well separated the model can identify uniquely all possible combinations of our 5 attributes. Indeed we observe in Fig. 14 some amount of color separation for the TCN but not for the baseline.



Figure 14: **t-SNE colored by attribute combinations:** TCN (bottom) does a better job than ImageNet-Inception (top) at separating combinations of attributes.

B. Pose Imitation Analysis



Figure 15: **t-SNE embedding before (top) and after (bottom) training, colored by view.** Before training, we observe concentrated clusters of the same color, indicating that the manifold is organized in a highly view-specific way, while after training each color is spread over the entire manifold.

C. Imitation Invariance Analysis

In this section, we explore how much invariance is captured by the model. In Fig. 18, we test the L2 imitation error from new viewpoints (30° , 90° and 150°) different from training viewpoints (0° , 60° and 120°). We find that the error increases but the model does not break down and keeps a lower accuracy than the Human model in Fig. 9. We also evaluate in Fig. 19 the accuracy while bringing the camera closer than during training (about half way) and similarly find that while the error increases, it remains competitive and lower than the human supervision baseline. From these experiments, we conclude that the model is somewhat robust to viewpoint changes (distance and orientation) even though it was trained with only 3 fixed viewpoints.



Figure 16: **t-SNE embedding before (top) and after (bottom) training, colored by agent.** Before training, we observe concentrated clusters of the same color, indicating that the manifold is organized in a highly agent-specific way, while after training each color is spread over the entire manifold.

D. Imitation Examples

t-SNE: We qualitatively evaluate the arrangement of our learned embedding using t-SNE representations with perplexity of 30 and learning rate of 10. In this section we show the embedding before and after training, and colorize points by agent in Fig. 16 and by view in Fig. 15. The representations show that the embedding initially clusters views and agents together, while after training points from a same agent or view spread over the entire manifold, indicating view and agent invariance.

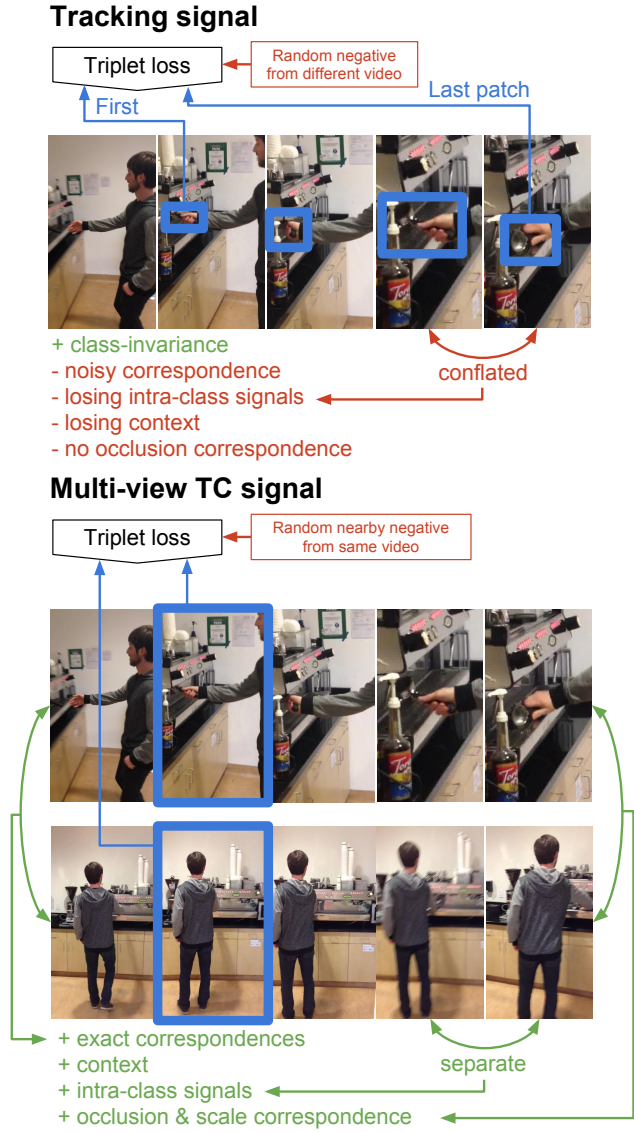


Figure 17: **Comparing temporal training signals** (e.g. [28]).

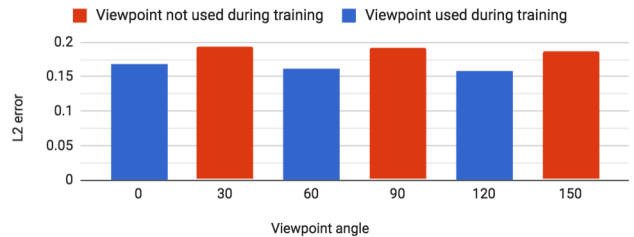


Figure 18: **Testing TC+Human+Self model for orientation invariance:** while the error increases for viewpoints not seen during training (30° , 90° and 150°), it remains competitive.

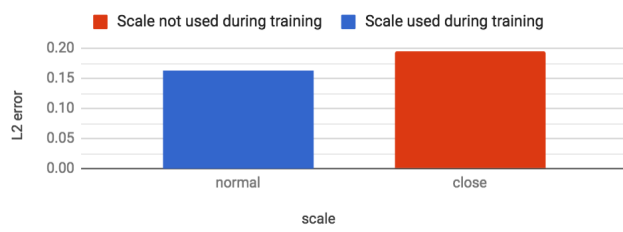


Figure 19: **Testing for scale invariance:** while the error increases when decreasing the distance of the camera to the subject (about half way compared to training), it remains competitive and lower than the human-supervised baseline.

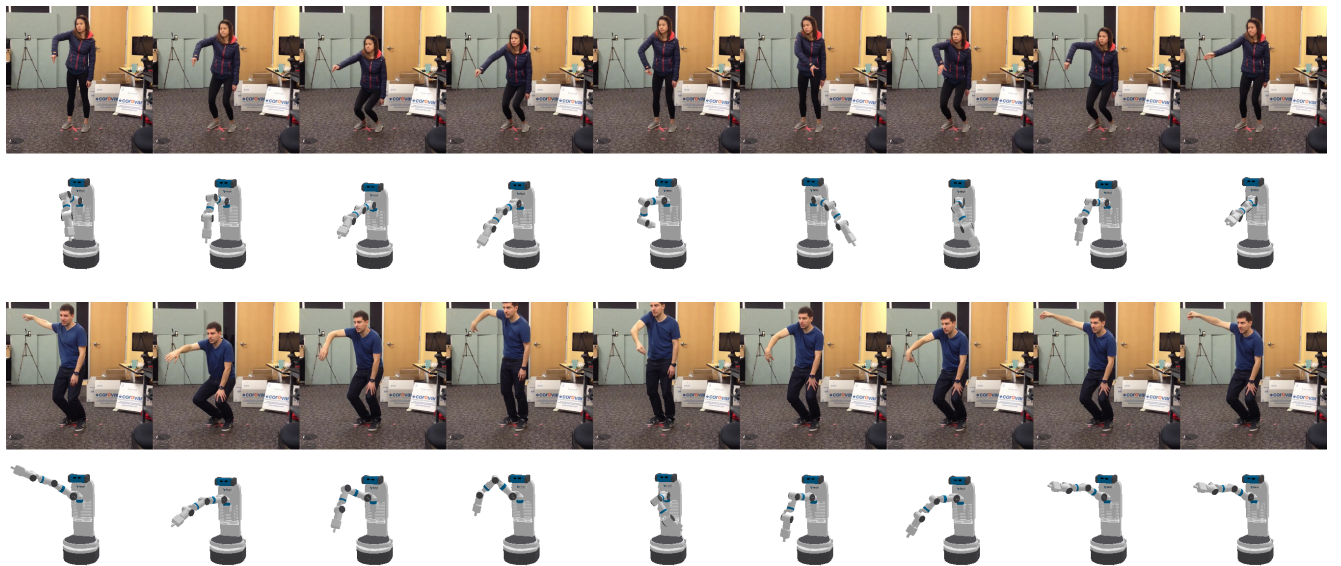


Figure 20: Self-supervised imitation examples. Although not trained using any human supervision (model "TC+Self"), the TCN is able to approximately imitate human subjects unseen during training. Note from the rows (1,2) that the TCN discovered the mapping between the robot’s torso joint (up/down) and the complex set of human joints commanding crouching. In rows (3,4), we change the capture conditions compared to training (see rows 1 and 2) by using a free-form camera motion, a close-up scale and introduction some motion-blur and observe that imitation is still reasonable.